Identification of a Subunit Interface in Transthyretin Amyloid Fibrils: Evidence for Self-Assembly from Oligomeric Building Blocks†

Ahmed A. Serag,‡ Christian Altenbach,§ Mari Gingery,|| Wayne L. Hubbell,§ and Todd O. Yeates*,⊥

Molecular Biology Institute, School of Medicine, Jules Stein Eye Institute, Department of Chemistry and Biochemistry, Department of Microbiology, Immunology, and Molecular Genetics, and Laboratory of Structural Biology and Molecular Medicine, Department of Energy, University of California, Los Angeles, California 90095

Received April 2, 2001; Revised Manuscript Received June 5, 2001

ABSTRACT: Amyloid and prion diseases appear to stem from the conversion of normally folded proteins into insoluble, fiber-like assemblies. Despite numerous structural studies, a detailed molecular characterization of amyloid fibrils remains elusive. In particular, models of amyloid fibrils proposed thus far have not adequately defined the constituent protein subunit interactions. To further our understanding of amyloid structure, we employed thiol-specific cross-linking and site-directed spin labeling to identify specific protein−protein associations in transthyretin (TTR) amyloid fibrils. We find that certain cysteine mutants of TTR, when dimerized by chemical cross-linkers, still form fibers under typical in vitro fibrillogenic conditions. In addition, site-directed spin labeling of many residues at the natural dimer interface reveals that their spatial proximity is preserved in the fibrillar state even in the absence of cross-linking constraints. Here, we present the first view of a subunit interface in TTR fibers and show that it is very similar to one of the natural dimeric interchain associations evident in the structure of soluble TTR. The results clarify varied models of amyloidogenesis by demonstrating that transthyretin amyloid fibrils may assemble from oligomeric protein building blocks rather than structurally rearranged monomers.

The term amyloid refers to stable, insoluble, rod-like fibrils resulting from the extracellular deposition of normally soluble proteins, or fragments thereof (*1*). The self-assembly of alternative conformations of proteins into fibrillar form is strongly implicated in a variety of neurodegenerative disorders, including Alzheimer's disease and prion-related encephalopathies (*2*−*4*). Despite the absence of sequence similarity among the growing family of amyloidogenic proteins, fibrils from different sources appear to share some structural properties (*5*). The main feature is a common core structure in which continuous β-sheets lie parallel to the long axis of a fiber, while their constituent β-strands run perpendicular to this axis (Figure 1). Although widely studied by electron microscopy, solid-state nuclear magnetic resonance, and X-ray fiber diffraction, finer structural details remain unclear because of the noncrystallinity and the insolubility of amyloid. In particular, models of amyloid fibrils proposed thus far have suffered from a lack of critical information about how individual protein subunits contact each other in an assembly.

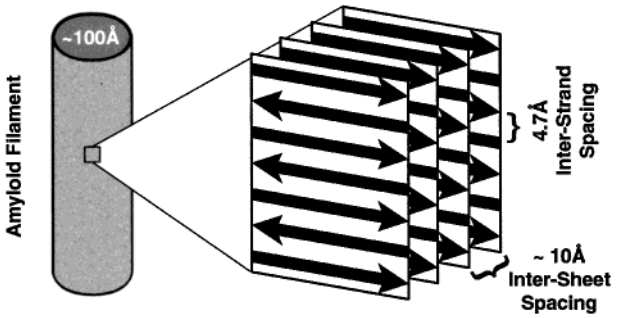

FIGURE 1: "Cross-β" model of amyloid fibrils. A variety of amyloids share a common morphology, presented here as a rod-like structure approximately 100 Å in width and of indefinite length. Current models of amyloid fibrils invoke a core of extended β-sheets organized such that the sheet is parallel to the long axis of the fiber, with the constituent β-strands perpendicular to this axis (*13*, *47*, *48*). Various models differ with respect to the number of sheets composing this core, and the distinction between a parallel or antiparallel arrangement of strands.

The protein transthyretin (TTR)[1] and its associated human amyloidoses have served as a model system for amyloidogenesis. In plasma and cerebrospinal fluid, the physiologically active tetramer of TTR (Figure 2A) transports thyroid

† This work was supported by NIH Grant GM31299 and NIH NIGMS Training Grant GM08042, and by DOE Grant DE-FC03-87ER60615. A.A.S. was supported in part by the Medical Scientist Training Program of the UCLA School of Medicine.

* To whom correspondence should be addressed. Phone: (310) 206-4866. Fax: (310) 206-3914. E-mail: yeates@mbi.ucla.edu.

‡ Molecular Biology Institute and School of Medicine.

§ Jules Stein Eye Institute and Department of Chemistry and Biochemistry.

|| Department of Microbiology, Immunology, and Molecular Genetics.

⊥ Laboratory of Structural Biology and Molecular Medicine, Department of Energy, and Department of Chemistry and Biochemistry.

[1] Abbreviations: TTR, transthyretin; SSA, senile systemic amyloidosis; FAP, familial amyloid polyneuropathy; PCR, polymerase chain reaction; SDS−PAGE, sodium dodecyl sulfate−polyacrylamide gel electrophoresis; ESI-MS, electrospray ionization mass spectrometry; OD, optical density; UV, ultraviolet; EM, electron microscopy; BMOE, bis(maleimido)ethane; BMB, 1,4-bis(maleimido)butane; $BM[PEO]_3$, 1,8-bis(maleimido)triethylene glycol; BMH, 1,6-bis(maleimido)hexane; $BM[PEO]_4$, 1,11-bis(maleimido)tetraethylene glycol; EPR, electron paramagnetic resonance; SDSL, site-directed spin labeling.

10.1021/bi010655s CCC: $20.00
Published on Web 07/12/2001

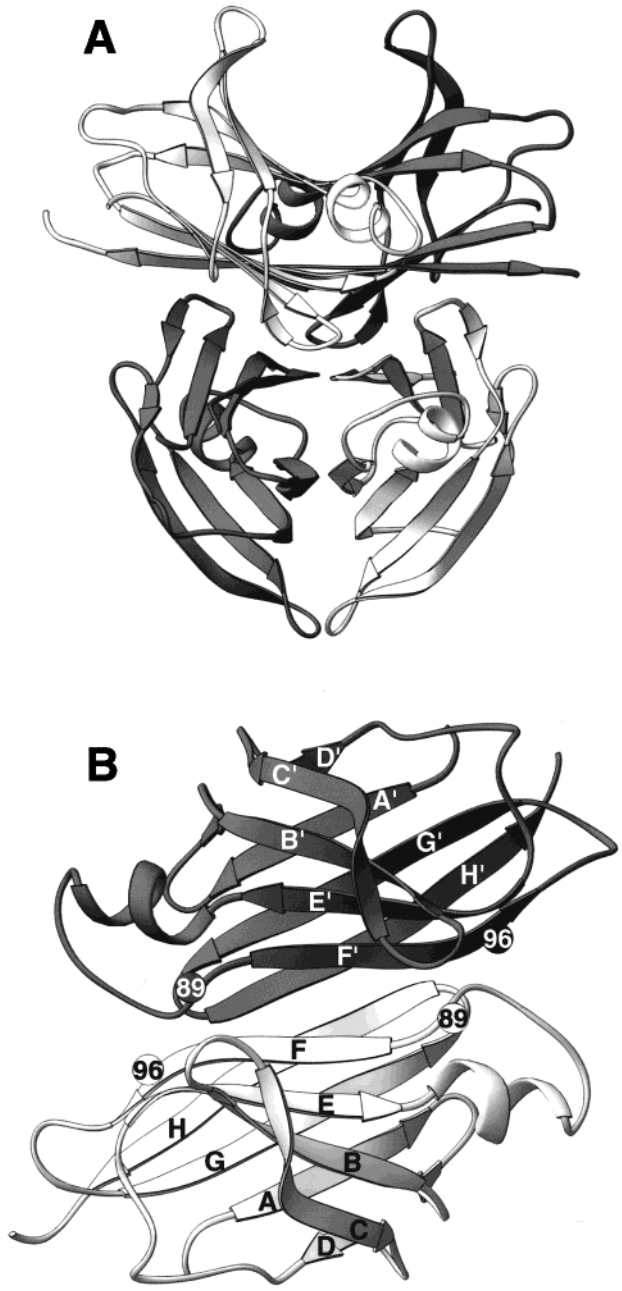

FIGURE 2: Three-dimensional structure of transthyretin (TTR). (A) Native TTR exists as a tetramer of identical 127-residue subunits, each containing extensive β-sheet structure. The ribbon diagram of the tetramer illustrates a dimer of dimers. (B) A view along one of the three molecular 2-fold axes of symmetry reveals that monomers dimerize through interchain interactions between both β-sheets of each monomer. Residues 89 and 96 in each monomer are labeled for reference; their C_α atoms are ~23 Å apart on the same monomer and ~7 Å apart between subunits. This figure were generated using PDB entry 2PAB (*49*) and the program RIBBONS (*50*).

hormones and vitamin A, the latter through a complex with retinol binding protein (*6*). In a condition known as senile systemic amyloidosis (SSA), wild-type TTR changes conformation and self-assembles into life-threatening cardiac fibrils. SSA is a late onset disease, affecting more than 25% of individuals who are more than 80 years old (*7*). In the autosomal dominant disorder familial amyloid polyneuropathy (FAP), a variety of more than 50 single-site variants of TTR deposit systemically. FAP generally manifests at an earlier age as a severe sensory, motor, and autonomic neuropathy. TTR fibers that form in vivo can be replicated in vitro under acidic, partially denaturing conditions, perhaps mimicking those inside a lysosome (*8*). Extensive biochemical and biophysical studies by Kelly and co-workers have illuminated some of the mechanistic details of TTR fibril formation (*9*−*12*). At low pH, the native tetrameric structure of transthyretin appears to dissociate to a monomeric amyloidogenic intermediate having a defined but non-native tertiary structure capable of self-assembly in vitro. The assembly of protein subunits into mature amyloid fibrils could also involve intermediate structures of increasing complexity (*13*−*16*).

In one popular model, an individual protein chain acts as the building block of TTR fibers (*17*). However, the three-dimensional structure of soluble TTR hints at an alternative mechanism. In Figure 2B, the dimer appears to contain two intermolecular eight-stranded β-sheets, CBEFF′E′B′C′ and DAGHH′G′A′D′, consistent with the continuous β-sheets envisioned for amyloid. The semblance of continuous intermolecular β-sheets suggests that some aspects of the natural dimeric association could be retained in the fibrillar form. The possibility that TTR fibrils could be built from dimeric building blocks was recognized by Blake and Serpell (*18*). Recently, Eneqvist and co-workers have suggested that a tetramer (a dimer of dimers) may be the building block of transthyretin amyloid fibrils, based on molecular packings observed in the crystal structure of a highly amyloidogenic variant of TTR (*19*).

Although various models have been proposed for transthyretin fibers, none have adequately defined the interactions between TTR subunits in the fibrillar state. We asked two questions to address whether the natural dimer interface is at least partially conserved in TTR fibrils. Are certain chemically cross-linked, dimeric forms of TTR able to self-assemble into amyloid? Can the interchain interactions known to exist in the native structure be observed in fibers assembled from nitroxide spin-labeled subunits? In this study, we provide affirmative answers to both of these questions. Taken together, the thiol-specific cross-linking and spin-labeling data suggest that one of the main subunit interaction types in the fibrillar state is very similar to one of the natural dimeric interchain associations. On the basis of these results, we propose a mechanism for fibrillogenesis involving an oligomeric intermediate that is either a dimeric building block or a multiple of such.

MATERIALS AND METHODS

Preparation of Cysteine Substitution Mutants. Transthyretin constructs were generated as described previously (*20*) with some modifications. The overlap-extension polymerase chain reaction (PCR) methodology was used to introduce cysteines at specific locations in a mutant of TTR in which the only native cysteine (residue 10) had been replaced with serine. Resulting PCR expression cassettes were cloned to contain noncleavable amino-terminal polyhistidine (six-His) tags. Transthyretin constructs were sequenced on both strands to ensure proper incorporation of cysteine-generating mutations. Recombinant TTRs were expressed in *Escherichia coli* [BL21(DE3)] and purified using nickel-affinity chromatography. Solutions of purified transthyretin protein were boiled in sample buffer (*21*) and analyzed by SDS−PAGE (12.5%

polyacrylamide gels). The faint bands corresponding to dimer are expected given that TTRs run as SDS-stable dimers on gels when samples are unboiled (*10*). Purified transthyretin mutants were further characterized by electrospray ionization mass spectrometry (ESI-MS) to ensure proper cysteine substitutions.

In Vitro Amyloid Fibril Formation. Stagnant protein solutions (1 mg/mL) were subjected to fibril forming conditions (pH 4.4 and 37 °C) as described previously (*10*) for 1 week. Incubated solutions were pelleted, washed three times by centrifugation followed by resuspension in distilled water, boiled in Laemmli sample buffer, and analyzed by SDS−PAGE as described above.

Light scattering was used to monitor amyloid fibril formation as a function of time. Optical density (OD) measurement at 330 nm in a standard UV cell was carried out on stationary TTR solutions incubated at 37 °C under fibrillogenic (pH 4.4) and nonfibrillogenic conditions (pH 7.2) over a time course of 1 week. Solutions of TTRs at pH 7.2 did show minor increases in the amount of light scattered over the incubation period; however, no visible aggregates or fibers were detected in any samples under this condition. Therefore, the extent of fibril formation was evaluated by

$$\Delta\Delta OD = [OD_{pH4.4}(t) - OD_{pH4.4}(t_0)] - [OD_{pH7.2}(t) - OD_{pH7.2}(t_0)]$$

The solutions were vortexed to equally distribute fibrils, if present, prior to each time point (t). Samples exhibiting an increase in $\Delta\Delta OD$ were also shown by spectrophotometry to bind Congo red and induce a hyperchromic effect and a red shift in the absorption maximum of Congo red, an attribute diagnostic of amyloid fibrils (*5*).

Electron microscopy (EM) was used to examine the gross morphology of putative fibrils. Carbon-coated parlodion support films mounted on copper grids were made hydrophilic immediately before use by high-voltage, alternating-current glow discharge. Samples presumed to contain fibrils, purified by three cycles of washing, were applied directly onto grids and allowed to adhere for 2 min. Grids were rinsed with distilled water and negatively stained with 1% uranyl acetate. Specimens were examined in a Hitachi H-7000 electron microscope at an accelerating voltage of 75 kV.

Thiol-Specific Cross-Linking. Chemical cross-linking of transthyretins using noncleavable cross-linking reagents (Pierce) was carried out as described previously (*22*). TTRs were exposed to the following sulfhydryl-reactive homobifunctional cross-linkers of differing flexible spacer arm lengths: bis(maleimido)ethane (BMOE), with a length of 8.0 Å; 1,4-bis(maleimido)butane (BMB), with a length of 10.9 Å; 1,8-bis(maleimido)triethylene glycol (BM[PEO]$_3$), with a length of 14.7 Å; 1,6-bis(maleimido)hexane (BMH), with a length of 16.1 Å; and 1,11-bis(maleimido)tetraethylene glycol (BM[PEO]$_4$), with a spacer arm 17.8 Å in length. The extent of chemical cross-linking was further determined by ESI-MS, and confirms that cysteines were covalently attached with approximately 75% efficiency. Solutions of TTRs exposed to cross-linkers were incubated to form fibrils and characterized as described above.

Spin Labeling and EPR Measurements. The sulfhydryl groups in the cysteine mutants were derivatized with a methanethiosulfonate spin-label to form the R1 side chain. Spin labeling of TTR mutants was carried out as described in ref *23* and verified by ESI-MS. The electron paramagnetic resonance (EPR) spectra of the resulting TTRs, both before and after incubation under fibril forming conditions, were obtained to identify dipolar-coupled nitroxide residues if present. In addition, the percent incorporation of the R1 side chain was measured after the incubation period and was not significantly different from that prior to fibrillogenesis. First-derivative absorption spectra were recorded on a Varian E-109 X-band spectrometer fitted with a loop-gap resonator (*24*). Spectra were collected at room temperature (20−22 °C) by signal averaging 16 scans over 200 G (1 G = 0.1 mT) using a microwave power of 2 mW and a modulation amplitude optimized to the natural line width of each individual spectrum. Portions of samples presumed to contain fibers, purified by three cycles of washing, were also assayed by Congo red binding to further ensure the integrity of the in vitro amyloid fibrils.

Calculation of the Inter-Nitroxide Distance. To assist in a quantitative analysis of interspin distances, an approximately isomorphous, magnetically silent analogue of R1, designated R1′, was used together with the paramagnetic side chain to obtain EPR spectra in the absence of spin−spin interaction as described in ref *23*. The electron paramagnetic resonance method for determining the distance between two site-specific nitroxides in the range of 5−25 Å is presented in ref *25*. Briefly, the EPR spectrum resulting from two interacting spins is treated as the convolution of the underlying spectrum (in the absence of magnetic interaction) with a broadening function (*26*). Here, a dipolar broadening function is approximated by a weighted sum of distance-dependent Pake (*27*) functions over a distribution of interspin distances.

RESULTS

Formation of TTR Fibrils from Cross-Linked Species. To create stable molecular dimers of transthyretin, mutants of TTR were designed with two key points in mind. First, the mutations were engineered to allow for site-specific chemical cross-linking between subunits. Second, it was important that the mutations not significantly affect amyloidogenesis by themselves. To satisfy these criteria, we introduced reactive cysteines at specific positions along strands F and H at the natural dimer interface. These site-directed mutations afforded covalent dimers of TTR using several noncleavable, thiol-specific cross-linking reagents. As described below, it was possible to form amyloid from various cysteine-containing constructs both before and after forced dimerization.

Figure 3 shows a mutant in which residues 89 and 96, neighbors in the dimer interface along the F and F′ strands (Figure 2B), were both mutated to cysteines (89C/96C). Prior to any cross-linking, experiments on the double-cysteine mutant were conducted to determine whether the cysteine substitutions had affected fibrillogenesis. The double mutant formed fibers under the same conditions as wild-type TTR. As expected, the soluble form of the un-cross-linked mutant protein and its resultant purified fibrils migrate primarily as monomers under denaturing, reducing conditions (Figure 3). The mutations appear to have little effect on the rate of fiber formation (Figure 4) or the morphology of the resultant fibrils

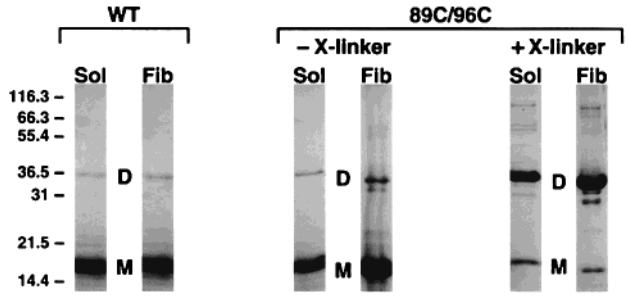

FIGURE 3: Irreversibly cross-linked species of TTR which self-assembles into amyloid fibrils. Samples of wild-type (WT) and a mutant TTR engineered to contain two cysteines at the dimer interface (89C/96C) were subjected to SDS−PAGE before (Sol) and after fibrillogenesis (Fib) as described in Materials and Methods. With wild-type TTR and the un-cross-linked mutant (−X-linker), the soluble proteins and their resultant fibrils migrate primarily as monomers (M) under reducing conditions. Cross-linking of the double mutant by BMH (+X-linker) yields a stable dimer (D) in solution. The cross-linked sample forms fibers which, when purified and analyzed by reducing SDS−PAGE, are confirmed to be built predominantly from dimers.

(Figure 5). Overall, with respect to formation of amyloid in vitro, the cysteine substitutions seem to be conservative.

The 89C/96C mutant was then cross-linked and incubated under fibril forming conditions to see if the dimerized mutant was able to self-assemble into amyloid. The double-cysteine mutant of TTR irreversibly dimerized after exposure to 1,6-bis(maleimido)hexane (BMH), a sulfhydryl-reactive chemical cross-linker with a flexible, noncleavable 16 Å spacer arm; ESI-MS confirmed that both pairs of cysteines were covalently attached by two BMH linkers (data not shown). The cross-linked double mutant formed fibers under the same conditions as native and un-cross-linked mutant TTRs. Moreover, fibers derived from the 89C/96C mutant appear to be built almost exclusively from dimers when analyzed by SDS−PAGE under reducing conditions (Figure 3). In addition to the double-cysteine mutant, the single-cysteine mutant 115C, which is at the dimer interface along the H and H′ strands, behaves similarly. Besides BMH, other cross-linkers with spacer arm lengths ranging from approximately 18 to 8 Å ($BM[PEO]_4$, $BM[PEO]_3$, BMB, and BMOE) afford dimeric TTRs that are fibrillogenic (data not shown). These results demonstrate that certain dimeric species, held together by covalent tethers, are competent to form fibers. Evidently, formation of free monomeric TTR is not an obligate step in fibrillogenesis.

Effect of Cross-Linking on Fibrillogenesis. Although analysis of the cross-linking experiments by SDS−PAGE suggests that dimerized TTR is still amyloidogenic, the use of cross-linked TTR raises possible concerns over whether the fibers formed are really genuine amyloid fibrils. To characterize the effect of thiol-specific cross-linking on the rate and extent of TTR fibrillogenesis, solutions of wild-type, un-cross-linked, and cross-linked variants of TTR were monitored by light scattering over the incubation period. Figure 4 shows that the rate of self-assembly for thiol cross-linked 89C/96C TTR is similar to that for wild-type and un-cross-linked forms. Although the "lag time" appears to be slightly extended in the case of the cross-linked variant, similar slight variations in lag time are observed between trials using strictly native proteins for fibril formation. In addition, the total mass of amyloid formed (as measured by turbidity) by cross-linked 89C/96C TTR is not significantly different from that formed using wild-type or un-cross-linked TTR. This suggests that although chemical cross-linking of TTR may mildly perturb the kinetics of amyloid fibril formation it does not alter the extent to which fibers are formed.

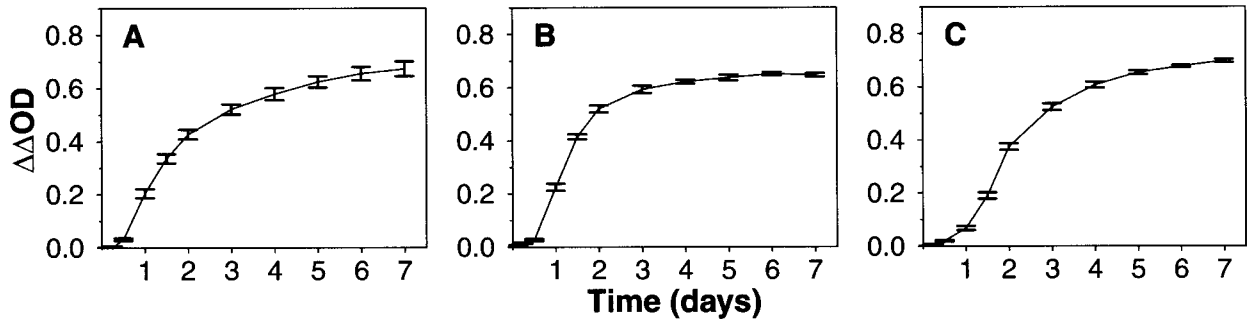

FIGURE 4: Chemical cross-linking of transthyretin has a negligible effect on the rate of fibrillogenesis. Light scattering was used to monitor fibrillogenesis as a function of time for (A) the wild type, (B) un-cross-linked 89C/96C, and (C) cross-linked double-cysteine mutant TTR. The extent of amyloid formation is expressed as ΔΔOD, the difference between the change in optical density from an initial time point at pH 4.4 and the baseline change in optical density under nonfibrillogenic conditions. Error bars are calculated as the standard error of the mean ($n = 3$).

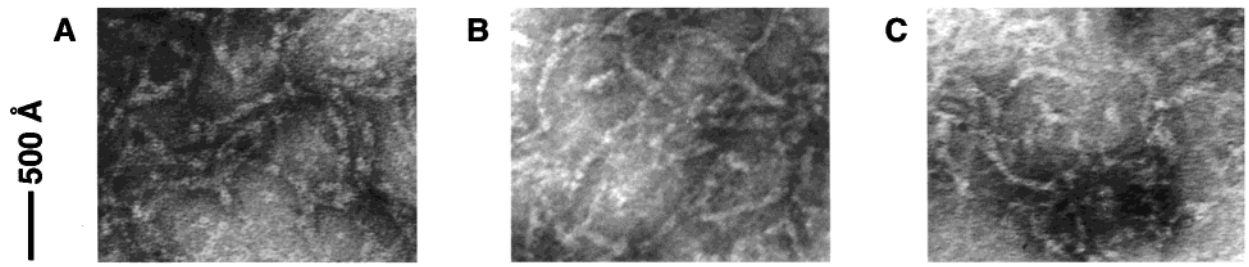

FIGURE 5: Chemical cross-linking of transthyretin has a negligible effect on the morphology of resultant fibrils. A comparison of electron micrographs of immature fibrils derived from (A) wild-type, (B) un-cross-linked, and (C) cross-linked transthyretin reveals amyloid of similar morphology. The scale bar is 500 Å in length.

To further ensure their integrity, fibers derived from certain cross-linked mutant TTRs were evaluated for standard dye binding and morphological properties of amyloid fibrils. The suspensions of purified fibers derived from wild-type, un-cross-linked, and cross-linked mutants of TTR were able to bind Congo red, which is characteristic of amyloid. Furthermore, the candidate fibrils were examined by electron microscopy (EM). Figure 5 shows that the morphologies of fibers derived from wild-type, un-cross-linked, and cross-linked 89C/96C TTRs are indistinguishable. Moreover, this morphology is no different from that typical of immature transthyretin amyloid fibrils, or protofilaments, as reported by others (*11*, *16*, *28*). It appears that cross-linking of TTRs across specific residues in the dimer interface has a negligible effect on the resultant fibrils. These results demonstrate that an oligomeric arrangement of TTR held together by covalent tethers can yield fibers representative of transthyretin amyloid.

Identification of a Dimeric Subunit Interface in Fibrils. To further demonstrate the presence of dimeric building blocks in fibers, site-directed spin labeling (SDSL) studies were undertaken to see if certain residues at the dimer interface remain in proximity in the fibrillar form without using chemical restraints. Here, we report a comparison of the electron paramagnetic resonance (EPR) spectra of mutants of TTR with spin-labels incorporated at the natural dimer interface, recorded before and after fibril formation. In addition, a quantitative analysis of interspin distances was undertaken by relating EPR spectra obtained in the presence and absence of spin−spin interactions. Given the dramatic broadening of resonance lines and the decrease in signal amplitudes resulting from interacting spins (*29*), an estimate of interspin distances could be made on the basis of a simulation of the broadened spectra assuming dipolar coupling (*25*).

The EPR spectra of spin-labeled mutants of TTR in the soluble state (prior to fiber formation) were obtained to confirm that spin−spin interactions could easily be detected across the dimer interface. The broadening of EPR spectra for several mutants identifies the expected natural dimer interface interactions (Figure 6). Broadening due to spin interaction causes a drop in amplitude (*23*, *25*, *29*). If the first derivatives of the absorption spectra are normalized to the same amplitude as shown in Figure 6, broadening is most visible as an apparent increase in the outer resonance line intensities of fully labeled (black spectra) versus magnetically dilute (red spectra) samples. Prior to fiber formation, the spectra for the single-cysteine mutant 90C reveal strong spin−spin interactions. This translates to a short interspin distance, as expected due to its location on the F and F′ strands (Figure 2B). The interspin distances calculated for other residues along the F strand (89C, 94C, and 96C) are larger than that for residue 90. This is expected since the 2-fold axis of symmetry is close to residue 92; TTR mutant 92C could not be spin-labeled due to its proclivity for spontaneous disulfide bond formation. In addition, strong interactions are observed for the double-cysteine mutant 89C/96C. According to the three-dimensional structure of soluble native TTR (Figure 2B), this interaction stems from 89R1 on one subunit coupled to 96R1 on the other subunit in the dimer.

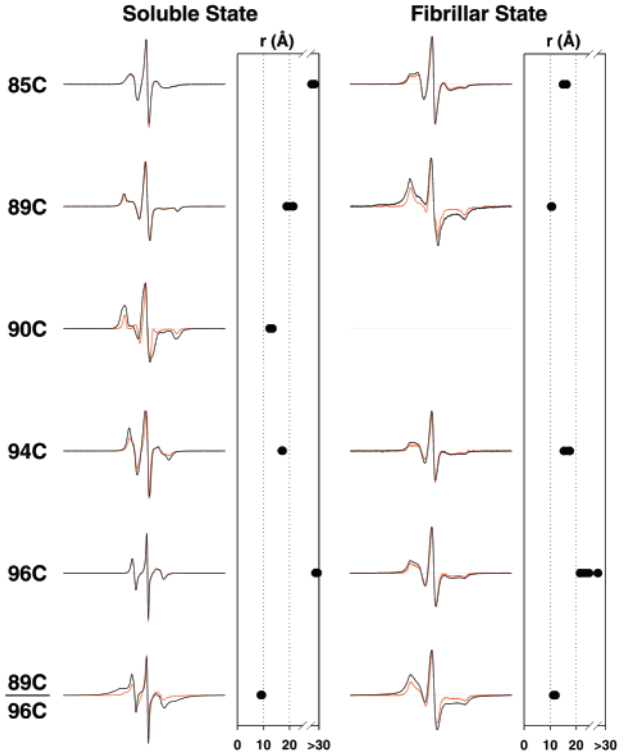

FIGURE 6: Site-directed spin labeling of soluble TTRs and transthyretin amyloid fibrils. In the soluble state, the spin labeling data are in good agreement with the crystal structure of TTR. As expected, the first-derivative absorption EPR spectra of the single-cysteine TTR mutants 89C and 96C show no evidence of interacting spins. In contrast, the spectrum of the double-cysteine mutant 89C/96C exhibits dipolar broadening prior to fiber formation, as expected. The calculated inter-nitroxide distances (*r*) prior to fibril formation correlate with known crystallographic data. The spectra obtained from purified fibers (formed from spin-labeled mutants) show spin−spin interactions that are similar in magnitude to those seen in the soluble state. In particular, for mutants 94C, 96C, and 89C/96C, the distances between nitroxides on corresponding residues from different subunits remain largely unchanged. An analysis of mutants 85C and 89C, before and after fibril formation, shows that the inter-nitroxide distances may be even shorter in the fiber than in solution. This supports the idea that the natural dimeric interface is preserved, if not somewhat strengthened, in the fibrillar form. The spectra of fully labeled (black) and magnetically dilute (red) samples are normalized relative to first-derivative amplitudes. Spectra were acquired at room temperature over 200 G as described in Materials and Methods.

EPR spectra were then repeated on suspensions of fibrils formed from these spin-labeled mutants to see if the spin−spin interactions across the natural dimer interface of soluble TTR were indeed preserved in the fibrillar state. The spectra of the TTR mutants in fibrillar form also clearly illustrate dipolar-coupled spins (Figure 6). Although the spectra obtained before and after fibril formation differ in detail, the inter-residue distances remain largely unchanged for mutants 94C, 96C, and 89C/96C. Unfortunately, analysis of the inter-nitroxide distance in the fibrillar state for TTR mutant 90C was not possible given its inability to form amyloid fibrils once it is spin-labeled. Given that the interspin distance for mutant 90C correlates with known crystallographic data prior to fiber formation, it is unlikely that spin labeling has grossly perturbed the native structure of the mutant of TTR. However, the presence of nitroxides at position 90 may result in a steric clash between subunits under fibrillogenic conditions, thereby making spin-labeled

TTR mutant 90C unfit to form amyloid. Nonetheless, the preservation of most spin−spin interactions provides further evidence that, in the fiber, the symmetry-related β-strands F and F′ of the dimer interface are still in proximity. In addition, novel interactions are gained upon fibril assembly, as can be seen from the decrease in inter-nitroxide distance determined for both residues 85 and 89. These novel spin−spin interactions could result from minor rearrangements in this region of the natural dimer interface that strengthen the subunit association or, alternatively, from additional subunit interfaces in the fiber; the data presented here are not able to discriminate between these two possibilities. Overall, the spin labeling results support the concept of a fiber built from dimeric building blocks.

DISCUSSION

TTR Amyloid Fibrils Can Assemble from an Oligomeric Intermediate. Whereas some earlier studies have implicated a monomeric intermediate in amyloidogenesis, our findings indicate that dissociation of the natural TTR tetramer to monomers is not necessary for fibril formation. Thiol-specific cross-linking experiments demonstrated that two different dimeric species of TTR are competent to form fibers. TTR dimers held together by either two covalent tethers spanning the F and F′ strands (double-cysteine mutant 89C/96C) or one spanning the H and H′ strands (single-cysteine mutant 115C) both self-assemble into fibrillar structures; the rate of formation, tinctorial properties, and morphology of fibrils built from these dimeric TTRs are similar to those for uncross-linked variants and wild-type transthyretin. The use of cross-linking agents with spacer arm lengths ranging from approximately 18 Å (BM[PEO]$_4$) to 8 Å (BMOE) suggests that the intimate association of TTR subunits across the natural dimer interface is reasonably preserved during fibrillogenesis.

The conclusions of the cross-linking studies were confirmed by less invasive means using site-directed spin labeling. In the absence of cross-linking constraints, nitroxide spin-labeled mutants self-assemble and reveal spin−spin interactions that can most easily be explained by subunit associations similar to those of the natural dimer interface. In addition to the preservation of many interprobe distances, notable decreases in inter-nitroxide distances are detectable near the subunit interface in the fibril, which suggests a strengthening of the natural interchain associations. Because the EPR measurements are carried out on purified fibers, as opposed to intermediates in the self-assembly pathway, the spin labeling studies provide the first view of a subunit interface in an amyloid fibril and one potential target for inhibiting fibrillogenesis (*30*−*32*).

Taken together, the thiol-specific cross-linking and SDSL data provide two independent lines of evidence for a self-assembly pathway involving an oligomeric intermediate that is either a dimeric building block or a multiple of such. The cross-linking and SDSL experiments independently argue that the F and F′ strands, found at the dimer interface of native soluble TTR, remain in proximity in transthyretin amyloid fibrils. Although the cross-linking of cysteine mutants across the dimer interface along the F and H β-strands has a negligible effect on TTR fibrillogenesis, the degree to which the native structure of TTR is preserved is not yet clear. While both short and long covalent tethers were used, we cannot disregard the likelihood of considerable structural changes in the native structure during fiber formation. Nonetheless, whatever conformational changes occur, it seems clear that they can be accommodated within the constraints of a dimeric structure whose interface is largely preserved.

Relationship to Previous Studies. Previous studies have led to varied models for TTR amyloid and its formation. Some models have implied assembly from monomeric intermediates (*17*), while others have allowed for or directly suggested that fibers are constructed from native-like oligomeric species (*19*). This range of views has left the existence of native-like oligomeric interactions in TTR fibers as an open question. We have addressed this issue as directly as possible and have found that a dimeric interaction is retained upon fiber formation.

Our conclusion that key aspects of the dimeric structure of TTR are conserved in the fibrillar form can be reconciled with other data that have favored a monomeric species as the key building block. For example, it is known that the monomer prevails at the low pH used to make fibers in vitro (*10*). In view of the present finding that a dimeric form of TTR can form fibers, the prevalence of a monomeric form can be explained as a secondary effect of the acidic conditions required in vitro to cause the conformational changes that must occur during amyloid formation. The low concentration of dimeric TTR observed during in vitro fibrillogenesis is consistent with a slow formation of oligomeric amyloidogenic building blocks, followed by their more rapid addition to growing amyloid fibers (*11*, *14*, *17*). The role of dimers was also called into question by an earlier finding that certain engineered disulfide-bonded dimers did not form fibers (*33*). However, given that conformational changes must occur, we would not expect all possible dimers to form fibers. By testing several possibilities, we have identified some dimers that do.

Our studies support the concept of a fiber built from dimeric building blocks. However, they do not rule out the possibility of assembly through a tetrameric intermediate, because the natural tetramer is essentially just two copies of the dimer. We have attempted to investigate the seemingly looser interface that holds two dimers together in native TTR, but have been unsuccessful because of insufficient spin labeling. A plausible tetramer-mediated mechanism for fiber formation has been proposed on the basis of the molecular packing in crystals of a highly amyloidogenic mutant of TTR (*19*). Although our findings of a dimeric building block do not rule out the involvement of a tetrameric species, they do clarify the issue of whether a monomer or an oligomer forms the core of TTR fibers (*18*). In general, the results of our cross-linking and spin labeling experiments lend more support to an emerging view that dimerization may play a significant role in the formation of filamentous assemblies from various proteins (*34*−*41*).

An Oligomer Model for TTR Amyloid Formation. The mechanistic details of in vitro TTR fibril formation are continuing to emerge from extensive biochemical and biophysical studies of low-pH intermediates along the self-assembly pathway and from examination of the structure of amyloid fibrils by microscopy and X-ray diffraction (*10*−*13*, *15*, *18*, *28*, *42*, *43*). The site-directed cross-linking and

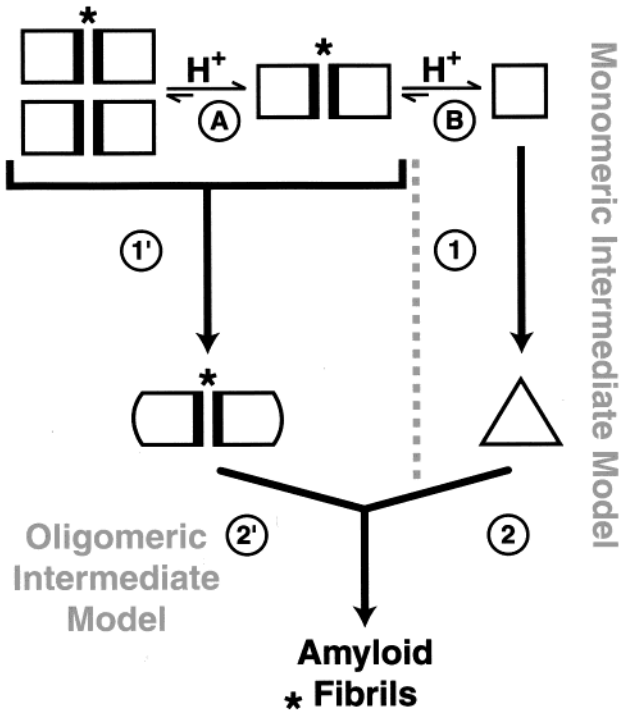

FIGURE 7: Monomeric vs oligomeric self-assembly pathways. TTR amyloid fibrils are generated in vitro by partial acid denaturation. With decreasing pH, the native tetrameric structure first dissociates to a dimer (step A) and then to a monomer (step B). According to the monomeric model for in vitro fibrillogenesis, TTR undergoes structural rearrangements (either during or after dissociation to monomer, step 1) resulting in a non-native monomeric intermediate that self-assembles into amyloid fibrils (step 2). Our findings support an oligomeric model for fibrillogenesis. Here, TTR undergoes structural rearrangements (step 1′) to afford an oligomeric intermediate, which may be a dimer or a tetramer. The oligomeric intermediate with a native-like dimeric interface (enhanced edges) ultimately forms amyloid fibrils through additional subunit interactions that have not been elucidated yet (step 2′). Spin labeling experiments on interface residues (∗) specifically confirm a partially preserved native-like dimeric interface in transthyretin amyloid fibrils.

spin labeling studies described here place new constraints on these evolving models of TTR amyloid fibrils and on the mechanism of their formation. While the results presented here do not lead to a complete picture of the TTR fibril, and do not strictly exclude the involvement of a monomeric species in TTR amyloidogenesis, they are more consistent with a different model. We propose one such model that preserves some of the native symmetry (Figure 7). Here, fibrillogenesis commences with a dimeric (or possibly tetrameric) building block that self-assembles, culminating in an amyloid fibril.

Whereas the natural dimer interface is partially conserved, additional subunit interfaces in the fiber most likely involve structural rearrangements in other regions of the TTR molecule. Notable conformational changes have been observed in studies of a solution state amyloidogenic intermediate (*42*, *43*). In addition, domain swapping has been implicated as one potential mechanism by which conformational change could lead to a new subunit interface in amyloid (*44*−*46*). While biophysical studies on soluble intermediates have furthered our understanding of the processes surrounding fibrillogenesis, direct structural information about the fibrillar state has been obtained only with difficulty due to the noncrystallinity and the insolubility of amyloid (*18*). As more SDSL experiments continue to probe the fibrillar state directly, additional subunit interactions will be identified and more complete models will illuminate the molecular basis for amyloid formation from TTR and other proteins.

Ultimately, the architectures of amyloid fibers must be dictated by geometric preferences in the way protein molecules tend to self-associate. Decades of crystallographic studies on soluble oligomeric assemblies have demonstrated that the quaternary structures of such complexes are dominated by a preference for symmetric arrangements, usually involving one or more dimeric associations. At issue is whether fibril-forming proteins are guided by similar or different principles of assembly. The evidence for symmetry in transthyretin fibrils suggests that the architectures of varied protein assemblies may be governed by similar rules and patterns.

ACKNOWLEDGMENT

We thank Jeffery Kelly, David Eisenberg, and Michael Lietzow for assistance and useful discussions.

REFERENCES

1. Sipe, J. D. (1992) *Annu. Rev. Biochem. 61*, 947.
2. Gajdusek, D. C. (1994) *Ann. N.Y. Acad. Sci. 724*, 173.
3. Perutz, M. F. (1996) *Curr. Opin. Struct. Biol. 6*, 848.
4. Kelly, J. W. (1997) *Structure 5*, 595.
5. Sunde, M., and Blake, C. (1997) *Adv. Protein Chem. 50*, 123.
6. Monaco, H. L., Rizzi, M., and Coda, A. (1995) *Science 268*, 1039.
7. Westermark, P., et al. (1990) *Proc. Natl. Acad. Sci. U.S.A. 87*, 2843.
8. Kelly, J. W., et al. (1997) *Adv. Protein Chem. 50*, 161.
9. Colon, W., and Kelly, J. W. (1992) *Biochemistry 31*, 8654.
10. Lai, Z., Colon, W., and Kelly, J. W. (1996) *Biochemistry 35*, 6470.
11. Lashuel, H. A., Lai, Z., and Kelly, J. W. (1998) *Biochemistry 37*, 17851.
12. Nettleton, E. J., et al. (1998) *J. Mol. Biol. 281*, 553.
13. Sunde, M., et al. (1997) *J. Mol. Biol. 273*, 729.
14. Lashuel, H. A., et al. (1999) *Biochemistry 38*, 13560.
15. Serpell, L. C., et al. (2000) *J. Mol. Biol. 300*, 1033.
16. MacPhee, C. E., and Dobson, C. M. (2000) *J. Mol. Biol. 297*, 1203.
17. Kelly, J. W. (1998) *Curr. Opin. Struct. Biol. 8*, 101.
18. Blake, C., and Serpell, L. (1996) *Structure 4*, 989.
19. Eneqvist, T., et al. (2000) *Mol. Cell 6*, 1207.
20. McCutchen, S. L., Colon, W., and Kelly, J. W. (1993) *Biochemistry 32*, 12119.
21. Laemmli, U. K. (1970) *Nature 227*, 680.
22. Wu, J., and Kaback, H. R. (1997) *J. Mol. Biol. 270*, 285.
23. Gross, A., et al. (1999) *Biochemistry 38*, 10324.
24. Hubbell, W. L., Froncisz, W., and Hyde, J. S. (1987) *Rev. Sci. Instrum. 58*, 1879.
25. Hubbell, W. L., Cafiso, D. S., and Altenbach, C. (2000) *Nat. Struct. Biol. 7*, 735.
26. Rabenstein, M. D., and Shin, Y. K. (1995) *Proc. Natl. Acad. Sci. U.S.A. 92*, 8239.
27. Pake, G. E. (1948) *J. Chem. Phys. 16*, 327.
28. Serpell, L. C., et al. (1995) *J. Mol. Biol. 254*, 113.
29. Hustedt, E. J., and Beth, A. H. (1999) *Annu. Rev. Biophys. Biomol. Struct. 28*, 129.

30. Miroy, G. J., et al. (1996) *Proc. Natl. Acad. Sci. U.S.A. 93*, 15051.
31. Peterson, S. A., et al. (1998) *Proc. Natl. Acad. Sci. U.S.A. 95*, 12956.
32. Klabunde, T., et al. (2000) *Nat. Struct. Biol. 7*, 312.
33. Redondo, C., Damas, A. M., and Saraiva, M. J. (2000) *Biochem. J. 348* (Part 1), 167.
34. Linke, R. P., et al. (1987) *Biol. Chem. Hoppe-Seyler 368*, 137.
35. Podlisny, M. B., et al. (1995) *J. Biol. Chem. 270*, 9564.
36. Ekiel, I., and Abrahamson, M. (1996) *J. Biol. Chem. 271*, 1314.
37. Garzon-Rodriguez, W., et al. (1997) *J. Biol. Chem. 272*, 21037.
38. Friedhoff, P., et al. (1998) *Biochemistry 37*, 10223.
39. Kuo, Y. M., et al. (1998) *Biochim. Biophys. Acta 1406*, 291.
40. Enya, M., et al. (1999) *Am. J. Pathol. 154*, 271.
41. Padilla, J. E., Colovos, C., and Yeates, T. O. (2001) *Proc. Natl. Acad. Sci. U.S.A. 98*, 2217.
42. Liu, K., et al. (2000) *J. Mol. Biol. 303*, 555.
43. Liu, K., et al. (2000) *Nat. Struct. Biol. 7*, 754.
44. Schlunegger, M. P., Bennett, M. J., and Eisenberg, D. (1997) *Adv. Protein Chem. 50*, 61.
45. Liu, Y., et al. (2001) *Nat. Struct. Biol. 8*, 211.
46. Janowski, R., et al. (2001) *Nat. Struct. Biol. 8*, 316.
47. Inouye, H., and Kirschner, D. A. (1997) *J. Mol. Biol. 268*, 375.
48. Tjernberg, L. O., et al. (1999) *J. Biol. Chem. 274*, 12619.
49. Blake, C. C., et al. (1978) *J. Mol. Biol. 121*, 339.
50. Carson, M. (1997) *Methods Enzymol. 277*, 493.

BI010655S